ELSEVIER

Journal of Nuclear Materials 296 (2001) 61–65

journal of nuclear materials

www.elsevier.com/locate/jnucmat

Simulation of the implantation of recoils and displacement production in the 316 stainless steel mercury-container vessel at SNS

Y. Zheng [a], M.S. Wechsler [a,*,1], D.J. Dudziak [a], J.D. Hunn [b], L.K. Mansur [b]

[a] *North Carolina State University, Raleigh, NC 27695-7909, USA*
[b] *Oak Ridge National Laboratory, Oak Ridge, TN 37831-6151, USA*

Abstract

In this study, the focus is on the possible effect of mercury and transmuted atom recoils that are implanted into the wall of the stainless steel container vessel at SNS. Two computer codes were used: Los Alamos high energy transport (LAHET) and the stopping and range of ions in matter (SRIM). LAHET provided information of the energy distribution of the recoils upon bombardment. Also, SRIM simulated the transport of recoils through the mercury layer adjacent to the stainless steel wall and into the wall itself, and provided recoil and displacement concentration profiles in the wall. The calculated recoil and displacement concentrations in the near-surface region of the wall appear to be quite significant. The recoil and displacement concentrations per year at the surface are determined to be about 0.0015 recoil atoms/wall atom and about 17 dpa at the center of an incident proton beam. These concentrations fall to about one-half of the surface values at a penetration distance of about 0.1 μm, and the concentrations become negligibly small at 0.5 μm and beyond.

1. Introduction

The target station at the SNS will include a multi-walled 316 stainless steel (316SS; Fe + 18 wt% Cr + 10 wt% Ni) vessel that contains the liquid mercury target material. Previous calculations of radiation damage (concentrations of displacements, helium, and hydrogen) to the 316SS have concentrated on the direct effect of bombardment by protons and spallation neutrons [1–4]. The innermost wall of the vessel has the main body of mercury target within it and mercury coolant surrounding it (see [1, Fig. 1] or [5, Fig. 5.3-6]), and both of these mercury bodies are bombarded by the incident 1 GeV protons. In this paper, we report on an investigation of displacement production in the 316SS due to mercury and transmutation products that recoil from reactions with the bombarding protons and become implanted into the 316SS wall.

Our approach is to calculate first the production of recoils that consist of mercury primary knock-on atoms (PKAs) and other transmutation products (which collectively we term 'recoils'). Then, the motion of these recoils to the 316SS wall is analyzed, and the depth dependence of the production rate for concentrations of recoil atoms and displacements is determined.

2. Computer codes

Two computer codes are used, Los Alamos high energy transport (LAHET) code, Version 2.82, and the stopping and range ions in matter (SRIM). LAHET or the LAHET code system [6] calculates the atomic number, mass number, energy, direction of motion, and point of origin of recoiling particles ejected from nuclear reactions, including intranuclear cascades and subsequent fission or evaporation. We ran the code in the default mode; by virtue of item IEVAP in LAHET, this

* Corresponding author. Tel.: +1-919 929 5193; fax: 1-919 933 6727.
E-mail address: wechsler@ncsu.edu (M.S. Wechsler).
[1] Present address: 106 Hunter Hill Place, Chapel Hill, NC 27514-9128, USA.

0022-3115/01/$ - see front matter
PII: S0022-3115(01)00500-1

means that the Rutherford Appelton Laboratory (RAL) evaporation–fission model was used [6–8]. HISTP within LAHET is a large history file that records the outcome of every particle event. LAHET also provides the post-processing HTAPE code. The option, IOPT 16, in HTAPE gives the energy spectrum of recoils (separately for elastic and inelastic interactions), and it uses the Lindhard model [9] to partition transferred energies into nuclear and electronic components. LAHET has now been merged with MCNP [10] into MCNPX [11,12].

The SRIM code can be down-loaded from the Internet [13], and it contains the transport of ions in matter (TRIM) code [14]. SRIM is a set of programs that calculate the stopping and range of ions with energy from 10 eV to 2 GeV/amu. In SRIM, the user specifies the ion and its energy and direction, and SRIM calculates target damage, sputtering, ionization, and phonon production. In particular, it calculates displacement concentration and its distribution. The Lindhard model [9] is used for partitioning the raw recoil energies into nuclear and electronic components.

3. Production of recoils

We ran LAHET and SRIM for 1 GeV protons on Hg to determine the recoil energy spectrum. For this purpose, we used 2.8×10^5 incident protons in LAHET and HTAPE with option IOPT 16. For SRIM we used 1×10^5 incident protons and the COLLISON.TXT file. The recoil spectrum data from the two codes were prepared with the same energy bin structure. The results are shown in Fig. 1. HTAPE IOPT 16 gave recoil distribution curves for elastic recoils and inelastic (or total) recoils. As Fig. 1 shows, the SRIM curve agrees roughly with the elastic recoil curve from LAHET, except below about 2 keV. This indicates that SRIM does not consider inelastic nuclear reaction events, whereas LAHET does. In our calculations, we adopted the total recoil energy distribution curve. This curve in Fig. 1 shows a change in slope at about 30 MeV, which corresponds to

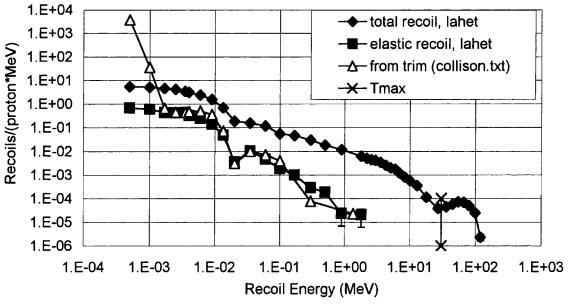

Fig. 1. Differential number of recoils per proton vs recoil energy for 1 GeV protons on mercury.

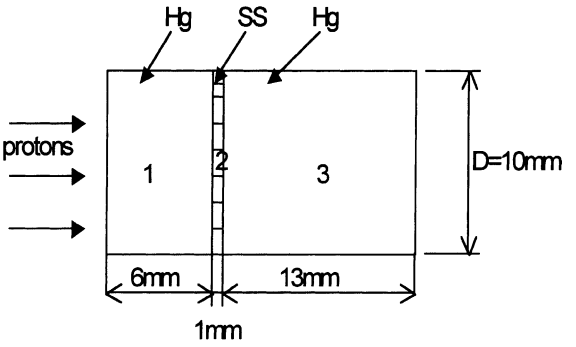

Fig. 2. Forward scattering model.

the maximum energy transfer for elastic collisions of 1 GeV protons on Hg of 30.2 MeV as calculated relativistically. This is indicated in Fig. 1 as T_{max}. The recoils of energies above 30 MeV are expected to stem largely from fission products. For the total recoil spectrum shown in Fig. 1, the fractional number of recoils with energies above $T_{max} = 30.2$ MeV is about 4%.

As mentioned above, the innermost wall of the target vessel has mercury on both the upstream and downstream sides. Accordingly, we have set up a forward scattering and a backscattering model. For the forward scattering model, as shown in Fig. 2, the vessel wall is represented by a 1 mm thick disk of 316SS surrounded by a 6 mm thick disk of Hg on the upstream side and a 13 mm thick Hg disk on the downstream side. For the backscattering model (Fig. 3), there is only a 13 mm thick Hg disk on the downstream side of the 1 mm thick disk of 316SS. For both models, the cross section perpendicular to the proton beam direction is a 10 mm diameter circle. According to SRIM, the range of 1 GeV protons in Hg is 44.8 cm. Therefore, the proton flux does not change much in traversing the Hg in the two models, and we can assume that the recoils generated by the incident protons are uniformly distributed throughout the Hg. The range of the 1 GeV protons in 316SS is 57.0 cm, so energy degradation in the steel is also negligible. In this paper, we deal only with the forward scattering

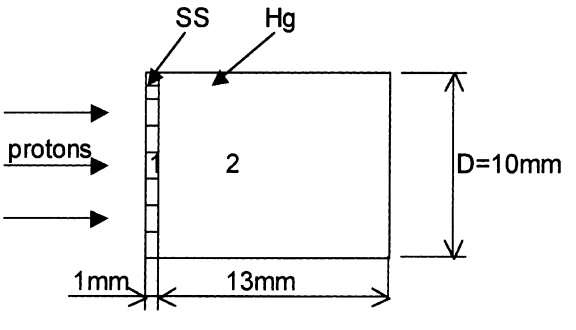

Fig. 3. Backscattering model.

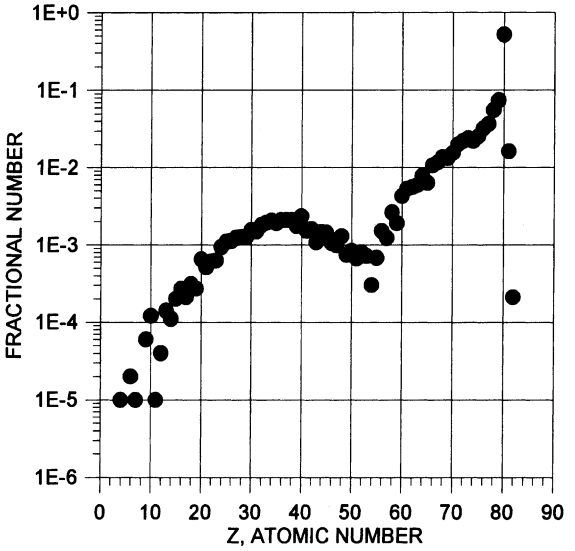

Fig. 4. Fractional number of recoils vs atomic number for 1 GeV protons on mercury.

model, which gives the greater amount of radiation damage.

The HTAPE option IOPT 8, detailed residual mass edit, gives information from which the fractional number of reaction products can be determined as a function of atomic number, Z. The result for 1 GeV protons on Hg is shown in Fig. 4. Mercury isotopes comprise about 51.6 atomic percent of the recoils. An additional 34.5 atomic percent corresponds to elements that lie within 10 atomic numbers from mercury, $Z = 80$.

4. Motion of recoils to the 316SS wall

As seen in Fig. 1, the maximum energy of the total recoil is about 110 MeV. From SRIM, the penetration range for 110 MeV mercury ions in mercury is found to be about 7.17 μm. Therefore, to make the calculation more efficient, we only consider recoils produced within 10 μm away from the 316SS wall, since the recoils generated outside this region cannot penetrate the mercury layer and reach the wall.

For each relevant recoil, the necessary starting information is Z, E, (X, Y, Z), and (U, V, W), where E is the recoil energy, (X, Y, Z) is the starting location, and (U, V, W) gives the direction cosines of motion. HTAPE does not provide information about (U, V, W). Three alternatives were studied with respect to (U, V, W):

1. Isotropic case: all directions chosen at random.
2. Unidirectional case: all recoils move toward the 316SS wall.
3. HISTP case: detailed recoil-by-recoil information used, as provided by HISTP.

For cases (1) and (2), as to E, a small program was written that extracts the energy distribution information provided by HTAPE option IOPT 16 and puts it in a form appropriate for input to SRIM. For (X, Y, Z), the coordinates were chosen randomly. As to Z, all recoils were assumed to be mercury. This is considered to be a reasonable assumption since, as stated above, a large fraction of the recoils were found to be adjacent to $Z = 80$. For case (3) where HISTP was used, the information of E, (X, Y, Z), (U, V, W), and Z were extracted from HISTP by another program. Thus, for case (3) the Z-numbers were those provided by LAHET and all of the recoils were not assumed to be Hg. Instead, the recoils were distributed in Z as given by Fig. 4.

5. Concentration of recoil atoms in the 316SS wall

The concentration of recoil atoms per wall atom per incident proton fluence is shown in Fig. 5 as a function of depth into the 316SS wall for the isotropic, unidirectional, and HISTP cases discussed above. Also shown is the corresponding concentration per year of beam-on exposure to the peak incident proton SNS flux of 1.40×10^{14} protons/cm^2 s. The curve for the unidirectional case shows the highest concentrations, but this is considered to be an extreme case, which provides only an upper limit. The HTAPE cases for 4×10^7 and 6×10^8 incident protons give concentrations in substantial agreement with the isotropic case. Since the

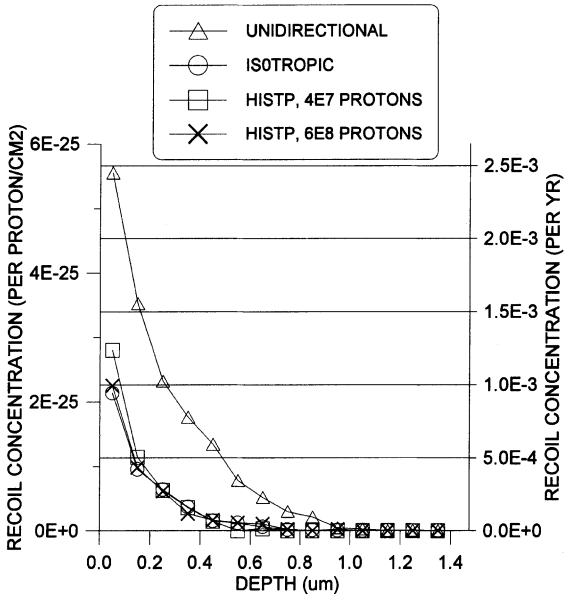

Fig. 5. Concentration of recoil atoms per wall atom per incident proton/cm^2 and per year vs depth into the 316SS wall. Bin width 0.1 μm.

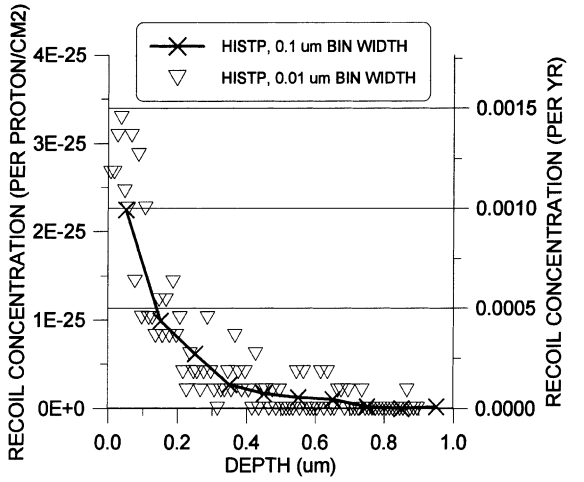

Fig. 6. Concentration of recoil atoms per wall atom per incident proton/cm^2 and per year vs depth into the 316SS wall. Bin widths 0.01 and 0.1 μm. Number of incident protons, 6×10^8.

recoils from nuclear reactions would tend to be isotropic, the agreement in recoil concentrations from the isotropic and HISTP cases is perhaps a reflection of the large contribution of inelastic nuclear reactions, as indicated in Fig. 1.

We note also, with respect to Fig. 5, that the penetration depth of the recoil atoms is quite short (less than 0.5 μm). In the attempt to obtain better definition for the curve of concentration vs depth, we decreased the bin width for the depth axis from 0.1 to 0.01 μm for the HISTP case. The result, shown in Fig. 6, indicates rather poor statistics for the data based on the 0.01 μm bin width, but it does suggest that the concentration at the surface of the 316SS may be about 0.0015 recoil atoms per stainless steel atom after a one-year exposure to the peak SNS proton flux of 1.40×10^{14} protons/cm^2 s.

6. Displacement production in the 316SS wall

As seen in Fig. 7, the curve of displacement concentration per unit proton fluence (dpa per proton/cm^2) or displacement production rate (dpa/yr) vs depth in the 316SS for the unidirectional case lies above those for the isotropic and HISTP cases. The curve for the isotropic case is in quite good agreement with the two HISTP curves using a bin width of 0.1 μm. For the HISTP case with 6×10^8 incident protons, Fig. 8 shows the displacement concentration and production rate based on bin widths of 0.01 and 0.1 μm. The extrapolation to the surface of the 316SS indicates a displacement production rate of about 17 dpa/yr for the peak SNS proton flux of 1.40×10^{14} protons/cm^2 s.

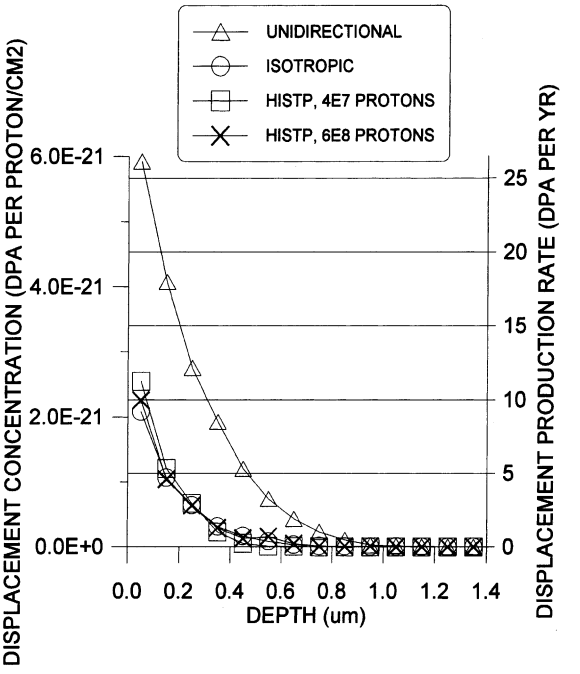

Fig. 7. Concentration of displacements per wall atom per incident proton/cm^2 and per year vs depth into the 316SS wall, based on peak incident flux of 1.40×10^{14} protons/cm^2 s. Bin width 0.1 μm.

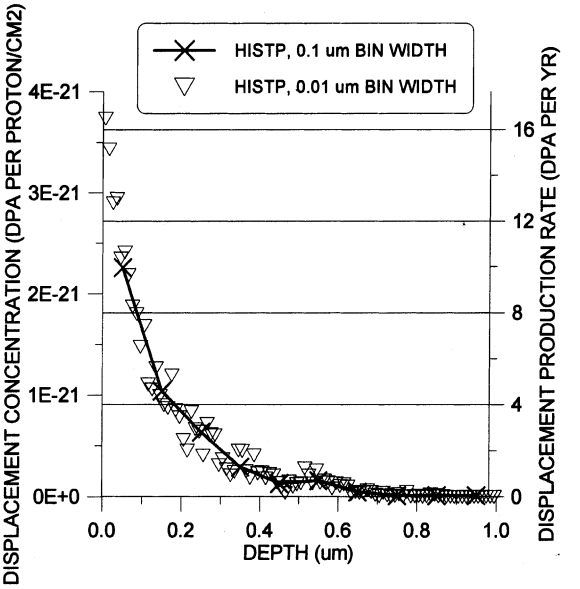

Fig. 8. Concentration of displacements per wall atom per incident proton/cm^2 and per year vs depth into the 316SS wall. Bin widths 0.01 and 0.1 μm. Number of incident protons, 6×10^8.

7. Discussion and summary

A preliminary analysis is presented of the concentrations of recoil atoms and displacements per proton/cm^2 due to the deposition of recoiling atoms in a 316SS wall adjacent and downstream of a layer of mercury irradiated by 1 GeV protons. At the surface of the 316SS wall, the corresponding production rates based on an incident proton flux of 1.40×10^{14} protons/cm^2 s (the flux anticipated at the center of the SNS proton beam) are estimated to be about 0.0015 recoiled atoms per metal atom per year and 17 dpa/yr and the penetration depth is about 0.5 μm. These rates assume that all the time is spent under beam-on conditions.

As pointed out in [4], the displacement production rate due to the direct effect of protons and spallation neutrons is calculated to be aout 36 dpa/yr where the center of the SNS beam strikes the nose of the innermost shell of the target container vessel. Thus, the calculations described here suggest that the deposition of recoil atoms from the mercury adjacent to the vessel wall could constitute a significant addition to the direct radiation damage.

There is the need, however, to confirm (or deny) the results described here with further, more comprehensive, calculations. Increased computer capacity would help considerably to reduce the statistical error in calculations devoted to the problem. This is the case since only a small fraction of the recoils produced in the mercury layer can reach the 316SS wall. In addition, we were not able to determine which species of elements, from among the many produced upon the 1 GeV proton bombardment (as shown in Fig. 4), were responsible for which part of the displacements produced. We hope these short-comings can be remedied in future studies.

References

[1] M.S. Wechsler, M.H. Barnett, D.J. Dudziak, L.K. Mansur, L.A. Charlton, J.M. Barnes, J.O. Johnson, in: M.S. Wechsler, L.K. Mansur, C.L. Snead, W.F. Sommer (Eds.), Materials for Spallation Neutron Sources, The Minerals, Metals, and Materials Society (TMS), Warrendale, PA, 1998, p. 23.

[2] M.H. Barnett, M.S. Wechsler, D.J. Dudziak, R.K. Corzine, L.A. Charlton, L.K. Mansur, in: Proceedings of the Third International Topical Meeting on Nuclear Applications of Accelerator Technology (AccApp99), American Nuclear Society, La Grange Park, IL, 1999, p. 555.

[3] L.A. Charlton, L.K. Mansur, M.H. Barnett, R.K. Corzine, D.J. Dudziak, M.S. Wechsler, in: Proceedings of the Second International Topical Meeting on Nuclear Applications of Accelerator Technology (AccApp'98), American Nuclear Society, La Grange Park, IL, 1998, p. 247.

[4] M.H. Barnett, M.S. Wechsler, D.J. Dudziak, L.K. Mansur, B.D. Murphy, these Proceedings, p. 54.

[5] Conceptual Design Report, National Spallation Neutron Source, vols. 1 and 2, NSNS/CDR-2/V1, NSNS/CDR-2/V2, Oak Ridge National Laboratory, Oak Ridge, TN, May 1997.

[6] R.E. Prael, H. Lichtenstein, User Guide to LCS: The LAHET Code System, LA-UR 89-3014, Radiation Transport Group, Los Alamos National Laboratory, Los Alamos, NM, September 1989.

[7] F. Atchison, in: Targets for Neutron Beam Spallation Sources, Jül-Conf-34, Kernforschungsanlage Jülich GmbH, January 1980.

[8] R.E. Prael, in: Proceedings of a Specialists Meeting, Issyles-Moulineaux, France, May 30–June 1, 1994, Intermediate Energy Nuclear Data: Models and Codes, OECD, 1994, p. 145.

[9] J. Lindhard, V. Nielsen, M. Scharff, P.V. Thomsen, Integral Equations Governing Radiation Effects, Notes on Atomic Collisions, III. Kongelige Danske Videnskabernes Selskab, Matematisk-Fysiske Meddelelser, vol. 33, No. 10, Copenhagen, 1963.

[10] J. F. Briesmeister (Ed.), MCNP – A General Monte Carlo Code for Neutron and Photon Transport, Version 4B, Los Alamos National Laboratory, March 1997, Los Alamos National Laboratory, Los Alamos, NM, 1997 (see also, Report LA-12625-M).

[11] H.G. Hughes, K.J. Adams, M.B. Chadwick, J.C. Comly, L.J. Fox, H.W. Egdorf, S.C. Frankle, J.S. Hendricks, R.C. Little, R. MacFarlane, R.E. Prael, L.S. Waters, M.C. White, P.G. Young, F.X. Gallmeier, E.C. Snow, in: Second International Topical Meeting on Nuclear Applications of Accelarator Technology (AccApp98), American Nuclear Society, La Grange Park, IL, 1998, p. 281.

[12] H.G. Hughes, K.J. Adams, M.B. Chadwick, J.C. Comly, S.C. Frankle, J.S. Hendricks, R.C. Little, R.E. Prael, L.S. Waters, P.G. Young Jr., in: Proceedings of the Topical Meeting on Nuclear Applications of Accelerator Technology, American Nuclear Society, La Grange Park, IL, 1997, p. 213. See also, H.G. Hughes, R.E. Prael, R.C. Little, MCNPX – The LAHET/MCNP Code Merger, Technical Report, XTM-RN (U) 97-012, Los Alamos National Laboratory, Los Alamos, NM, April 1997.

[13] http://www.research.ibm.com/ionbeans/SRIM.

[14] J.F. Ziegler, J.P. Biersack, U. Littmark, The Stopping and Range of Ions in Solids, Pergamon, New York, 1985.